• Investigation •

Fractal analysis of retinal vasculature in normal subjects on ultra-wide field fluorescein angiography

Wen–Ying Fan[1,2,3], Alan Fleming[4], Gavin Robertson[4], Akihito Uji[2,3], Jano van Hemert[4], Michael Singer[5], Min Sagong[2,3], Michael Ip[2,3], SriniVas R. Sadda[2,3]

[1]Beijing Tongren Eye Center, Beijing Tongren Hospital, Beijing Ophthalmology and Visual Sciences Key Laboratory, Capital Medical University, Beijing 100730, China

[2]Doheny Image Reading Center, Doheny Eye Institute, Los Angeles, CA 90086, USA

[3]Department of Ophthalmology, David Geffen School of Medicine at UCLA, Los Angeles, CA 90095, USA

[4]Optos PLC, Dunfermline KY11 8GR, United Kingdom

[5]Department of Ophthalmology, Medical Center Ophthalmology Associates, San Antonio, TX 78258, USA

Correspondence to: SriniVas R. Sadda. Doheny Eye Institute, PO Box 86228, Los Angeles, CA 90086, USA. ssadda@doheny.org

Received: 2020-01-06   Accepted: 2020-02-12

Abstract

● **AIM:** To evaluate the fractal feature of the retinal vasculature of normal eyes on a stereographic projected and montaged ultra-wide field (UWF) fluorescein angiography (FA).

● **METHODS:** Prospective, observational, cross-sectional study. Totally 59 eyes of 31 normal subjects were imaged using the Optos 200Tx. Images obtained at different gaze angles stereographically projected and montaged. The early-phase UWF FA frames were processed to segment the retinal vasculature and the results were exported as binary masks. The fractal dimension (FD) was calculated using the box-counting method.

● **RESULTS:** The global FD for the entire retina was 1.6 ± 0.04, with no difference between males and females (1.59 ± 0.04 *vs* 1.61 ± 0.04, $P=0.084$) or between right and left eyes (1.6 ± 0.04 *vs* 1.6 ± 0.05, $P=0.61$). FD was non-uniformly distributed among four quadrants ($P<0.001$) and decreased as the distance from the fovea increased ($P<0.001$). A negative association was observed between FD and age ($R=-0.37$, $P=0.006$), and this relationship was observed in the posterior and mid-peripheral retina ($P<0.05$) but absent in far-periphery ($P>0.05$).

● **CONCLUSION:** Fractal geometry is non-uniformly distributed across the retina in normal eyes and decreases from the fovea to the far-periphery. Subjects with an older age tend to have a smaller FD, however, the FD in the far-periphery does not appear to be influenced by age.

● **KEYWORDS:** fractal analysis; retina; ultra-wide field; fluorescein angiography; normal subject

INTRODUCTION

Ultra-wide field (UWF) fluorescein angiography (FA) has evolved into an important tool for the clinical care of patients with various retinal disorders[1-2]. The Optos 200Tx scanning laser ophthalmoscope (SLO; Optos PLC, Dunfermline, Scotland, UK) enables visualization of the entire fundus[3-4]. In addition, stereographic projection techniques have allowed peripheral image distortion to be corrected[5], facilitating accurate measurement of lesions and features of interest such as retinal non-perfusion area (NPA) and vascular area in square millimeters[6].

The retinal vasculature harbors a branching pattern that presents the property of self-similarity which can be considered a fractal structure[7]. Fractal analysis provides a global evaluation of the architecture of a vascular network using fractal dimension (FD), a single value between 1 and 2 on a 2-dimensional fundus image, with a higher value reflecting increased branching complexity as represented by the density of the space-filling pattern of the retinal vascular tree[8]. FD was observed not be affected by ocular magnification. Li *et al*[9] found no evidence supporting any refractive axial magnification effect on fractal analysis. Error in fractal measurements due to retinal curvature was reported to be small (approximately 3%)[10]. Therefore, in contrast to the measurement of lesion size (*e.g.* area of linear dimension), fractal analysis appears to be less dependent on the need for correcting peripheral distortion, which may be of importance where stereographic projection algorithms cannot be applied. In addition, fractal analyses are more easily performed

automatically and may obviate the need for manual grading for the assessment of retinal vascular diseases.

Several studies have performed fractal analysis in healthy or diseased retina using fundus photographs and optical coherence tomography angiography (OCTA)[8,11-12]. In addition to limitations such as artifact (motion, projection) and segmentation error in OCTA[11] or the insufficient demonstration of microvasculature on color photographs[12], these studies were mostly limited to small regions around the optic disc (OD) or macula, and thus did not evaluate attributes of the peripheral retina. Multiple studies, however, have demonstrated the relevance of peripheral lesions to various retinal diseases and their correlation with disease severity[1,13-14]. Thus, there is a lack of a study that quantified the global FD for the entire retina on UWF images and characterized its regional distribution in normal or diseased eyes.

Previously we have reported on total visible retinal area and retinal vascular density (VD) in a cohort of healthy subjects (age range: 20-73y) who underwent UWF FA examination[4]. In the present study we aim to provide normative data on FD from stereographically projected and montaged UWF FA images.

SUBJECTS AND METHODS

Ethical Approval This prospective observational study was conducted at the Medical Center Ophthalmology Associates, San Antonio, Texas, and was approved by its institutional review board. This study adhered to the tenets of the Declaration of Helsinki. Written informed consent was obtained from all subjects before imaging.

The study protocol has been described in detail in previous reports[4]. Fifty-nine eyes of 31 healthy subjects were included in the Study.

Image Acquisition, Projection and Montage The methods of image acquisition, projection and montage have been reported in detail in our prior study[4].

After intravenous administration of fluorescein dye, UWF FA images were captured using the Optos 200Tx (Optos plc, Dunfermline, United Kingdom)[4].

Images were collected and sent to the Doheny Image Reading Center (Doheny Eye Institute, Los Angeles, California, USA) for analysis. Images transformed by stereographic projection allowed measurements of pixel area to be converted to square millimetre, and this conversion varied with distance from the fovea[15] (Figure 1A).

Segmentation and Skeletonization of Retinal Vasculature The early-frame of the UWF FA angiogram sequence (4000×4000 pixels) was selected to segment the retinal vasculature. Images were excluded where insufficient contrast between the retinal vasculature and the background fluorescence prevented retinal vessel segmentation. The
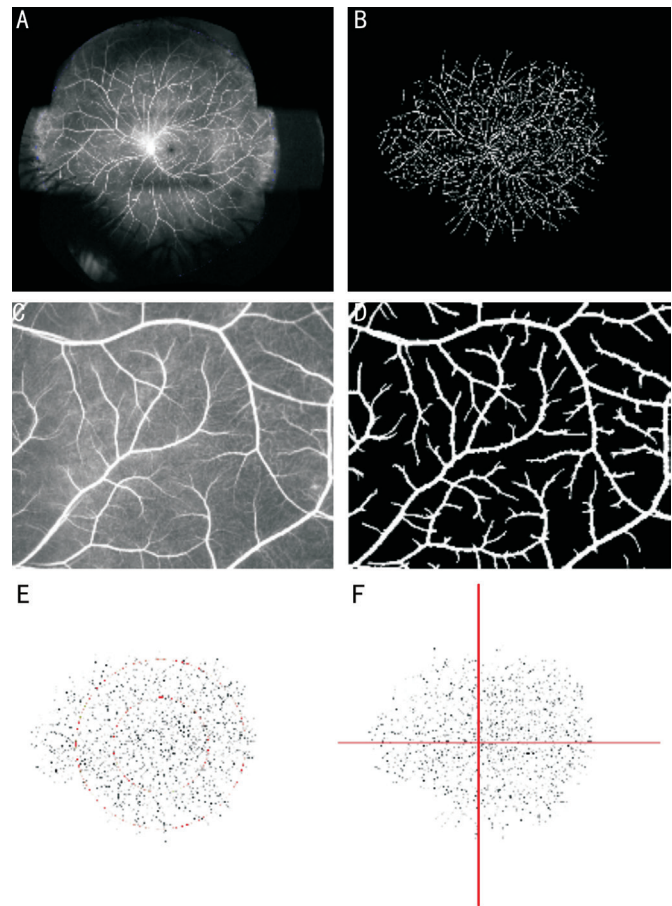
Figure 1 Retinal vessels on a montaged ultra-wide field fluorescein angiography (UWF FA) image of a normal subject A: A montaged UWF FA image of a normal subject; B: Binarized image of retinal vasculature on A; C: A cropped area of A; D: Binarized image of C. It enables a clear delineation of the vessels with large, medium, and small caliber, as well as the large diameter capillaries, but little visualization of the smaller capillaries. E: The skeletonized image of retinal vasculature on B; The retina on UWF FA was divided into 3 pre-specified zones; F: The skeletonized image of retinal vasculature on B. The retina was divided into four quadrans centered at optic disc: supero-temporal quadrant; infero-temproal quadrant; supero-nasal quadrant; infero-nasal quadrant.

algorithm for vessel segmentation was described in detail in a prior study which was performed on UWF pseudocolor images[16]. The segmented retinal vasculature were converted into binary masks (Figure 1B, 1D). Each binary imaging was then skeletonized by decreasing each continuous white segment to a line of single pixel width using Image J (National Institutes of Health, https://imagej.nih.gov/ij/; Figure 1E and 1F).

Division of Retinal Field The method of retinal field division has been established in prior study[6]. A pre-specified custom grid consisting of two rings or circles centered on the fovea was applied to each image, dividing it into three zones: a posterior zone (within a radius of 10 mm), a mid-peripheral zone (10-15 mm), and a far periphery zone (>15 mm; Figure 1E)[6]. In addition, based on the quadrantic arborization of the

major retinal vascular arcades, the retina was also divided into four quadrants centered on the center of the OD: supero-temporal, infero-temproal, supero-nasal, and infero-nasal quadrants (Figure 1F)[6]. After cropping, the images were saved as a bitmap for further regional calculation of FD[6].

Calculation of Fractal Dimension The method of FD calculation has been described in our prior study[17]. The resultant images were processed using Image J software with FracLac plugin (National Institutes of Health, https://imagej.nih.gov/ij/plugins/fraclac/fraclac.html) to calculate FDs using the box-counting method[17-18].

Statistical Analysis Statistical analysis was performed using the R statistical package (version 3.3.0). Difference between right and left eyes was tested using a paired sample t-test (normally distributed data) or Wilcoxon signed-rank test (non-normally distributed data). The independent t-test was performed to compare means for normally distributed data and nonparametric analysis (Wilcoxon rank sum test) was used for non-normally distributed data.

FD among the 4 quadrants or 3 circular zones were compared using a one-way analysis of variance test. Pearson correlation coefficient was used to describe the relationship between demographic features and FD. A Kruskal-Wallis test was performed to compare the 6 different age groups. Post hoc analysis was used to perform multiple comparisons between 2 groups. Statistical results were expressed as P-values and a P-value <0.05 was considered statistically significant.

RESULTS

Demographic Features of the Study Eyes at Baseline Of 59 eyes, 5 eyes were excluded because of insufficient contrast between the retinal vasculature and the background fluorescence in order for the retinal vessels to be segmented. Thus, 54 eyes were included in the final analysis. Demographic manifestations at baseline are presented in Table 1. The mean age was 45.3±16.1y (median, 46.5y; range, 20-73y; male: 57.4%), mean spherical equivalent was -0.6±1.8 diopters (D; median, -0.25 D; range, -7.25-2.25 D) and intraocular pressure (IOP) was 16.2±3.7 mm Hg (median, 16.5 mm Hg; range, 10-24 mm Hg). The mean systolic bolld pressure (BP) was 122.7±8.7 mm Hg (median, 121.8 mm Hg; range, 102-139 mm Hg) and mean diastolic BP was 78.2±8.4 mm Hg (median, 79.8 mm Hg; range, 46-88 mm Hg; Table 1).

Fractal Dimension and Its Distribution The mean skeletonized FD was 1.6±0.04 for the global retina, with no difference in gender (1.59±0.04 vs 1.61±0.04 mm^2, P=0.084) or between right and left (1.6±0.04 vs 1.6±0.05, P=0.61) eyes (Table 2).

There were significant differences in FD among the various quadrants (P<0.001), with FD greater in the temporal compared nasal retina and inferior retina greater than superior

Table 1 Demographic features of patients and study eyes

Demographic features	Values
No. of eyes (No. of patients)	54 (29)
RE (Diopter)	-0.6±1.8
Age (y)	45.3±16.1
Sex (M/F)	31/23
Heart rate (times/min)	73.1±9.9
Systolic blood pressure (mm Hg)	122.7±8.7
Diastolic blood pressure (mm Hg)	78.2±8.4
Intraocular pressure (mm Hg)	16.2±3.7
Lens status (phakic/pseudophakia)	53/1
Laterality (right/left)	28/26

RE: Refraction error. Numeric data are presented as means±standard deviation unless otherwise indicated.

Table 2 Fractal dimension in different retinal region

Parameters	Fractal dimension	P
Circular zone		
Posterior zone (<10 mm)	1.58±0.06	< 0.001
Mid-periphery (10-15 mm)	1.5±0.06	
Far-periphery (>15 mm)	1.47±0.07	
Whole	1.6±0.04	
Quadrant		
Temporal-superior	1.5±0.07	< 0.001
Temporal-inferior	1.53±0.06	
Nasal-superior	1.46±0.07	
Nasal-inferior	1.46±0.08	
Gender		
Male (n=23)	1.59±0.04	0.084
Female (n=31)	1.61±0.04	
Laterality		
Right eye (n=28)	1.6±0.04	0.61
Left eye (n=26)	1.6±0.05	

Numeric data are presented as means±standard deviation unless otherwise indicated. Values of P (two-tailed) <0.05 was considered statistically significant.

retina (P<0.001). With respect to the fovea, FD decreased with the increasing distance from the fovea (P<0.001; Table 2).

Correlation of Demographic Features with Fractal Dimension Linear regression analysis showed that the mean FD for the entire retina was negatively associated with age (R=-0.37; P=0.006) and systolic BP (R=-0.4; P=0.003; Table 3). No associations were observed between FD and refractive error (RE), heart rate, diastolic BP, or IOP (P>0.05; Table 3).

Variations in Fractal Dimension According to Age The relationship between a decreasing FD and increasing age was present for the whole retina as well as in all retinal quadrants (Table 4; P<0.05). Pairwise comparisons showed that the mean FD in individuals older than 65y was significantly lower than those younger than 60y (Table 4; P<0.05). In subjects between

Table 3 Association between of demographic manifestations and fractal dimension

Demographic features	Fractal dimension	
	R	P
Refraction error	-0.19	0.179
Age of first visit	-0.37	0.006
Heart rate	0.15	0.294
Systolic blood pressure	-0.4	0.003
Diastolic blood pressure	-0.16	0.235
Intraocular pressure	0.09	0.539

P value were calculated using linear correlation modeling. Values of *P* (two-tailed) <0.05 was considered statistically significant.

Table 4 Fractal dimension in different retinal regions according to age in normal subjects

Sector	Fractal dimension by age range (y)						P
	20-29 (*n*=11)	30-39 (*n*=10)	40-49 (*n*=10)	50-59 (*n*=10)	60-65 (*n*=7)	>65 (*n*=6)	
Whole	1.62±0.02	1.61±0.04	1.6±0.05	1.6±0.03	1.6±0.05	1.54±0.04	0.008
TS	1.53±0.04	1.49±0.07	1.52±0.07	1.49± 0.05	1.53±0.08	1.43±0.05	0.022
TI	1.54±0.03	1.54±0.07	1.55±0.04	1.53±0.04	1.52±0.09	1.42±0.07	<0.001
NS	1.51±0.04	1.47±0.07	1.48±0.08	1.44±0.06	1.47±0.08	1.36±0.04	0.002
NI	1.49±0.05	1.46±0.07	1.49±0.06	1.48±0.03	1.46±0.10	1.33±0.09	<0.001
Posterior zone	1.61±0.03	1.6±0.03	1.57±0.07	1.6±0.02	1.52±0.08	1.54±0.07	0.003
Mid-periphery	1.53±0.03	1.52±0.04	1.49±0.05	1.52±0.02	1.46±0.08	1.43±0.09	0.002
Far-periphery	1.48±0.04	1.47±0.06	1.49±0.07	1.47±0.04	1.49±0.09	1.39±0.11	0.079

TS: Supero-temporal quadrant; TI: Infero-temproal quadrant; NS: Supero-nasal; NI: Infero-nasal.

20 to 65y of age, however, FD did not appear to be associated with age (*P*>0.05).

With respect to different circular zones, FD in the far-periphery with a radius of more than 15 mm from the fovea was not correlated with age, however, a decreasing FD with increasing age was present in the more posterior zones (<15 mm; Table 4).

DISCUSSION

In this study, we evaluated the fractal feature of the retinal circulation throughout the fundus in UWF FA images from healthy subjects. The FD had, for the whole retina, a mean of 1.6, had a non-uniform distribution among the different quadrants and decreased from the fovea to the far-periphery. A lower FD was correlated to an older age and a higher BP. Although the tendency for decreased FD with age was evident in all four quadrants and the posterior and mid-peripheral retina, it was not evident in the far periphery. A significant advantage of fractal analysis is that it is not dependent on correcting peripheral distortion. Also, our finding that FD was not correlated to RE was as expected.

The present study documented a mean FD of 1.6 for the entire retina, which is similar to the previously reported value of 1.7[7,19]. When comparing our results with those obtained by other imaging modalities, we observed that our FD value was higher than most values obtained from color fundus photographs[20-21], but largely lower than most OCTA studies[8,11,22]. Compared with color photographs, FA has conventionally been the gold standard imaging modality for

identifying and analyzing the retinal vessels, especially the capillary system[23]. Thus, it is not surprising that we observed a higher FD than that calculated on photographs. Although it is not surprising that OCTA reported a higher FD than ours due to the higher resolution and contrast of OCTA for displaying the microvasculatrue, the difference in FD between those two modalities was not considerble (1.6 *vs* approximate 1.64-1.74)[8,11,22]. Moreover, OCTA analysis is inevitably limited by projection artifact or segmentation errors when assessing the reliability of FD measurements[11]. In addition, small discontinuities in vessel segments in unaveraged OCTA images can confound FD measurements[24]. Avakian *et al*[18] also conducted fractal analysis using a box-counting method on 60° FA images in normal subjects and reported a smaller FD (1.46) than ours. This discrepancy may be ascribed to the vessel segmentation method. The protocol of vessel segmentation applied in the present study was particularly designed for UWFoV SLO images and has been shown to have good performance with regards to vessel segmentation accuracy and the lowest overall bias[16].

Our study demonstrated a non-uniform distribution of FD among different retinal quadrants, with a larger FD in the temporal retina compared to nasal, and larger FD in the inferior retina compared to superiorly. Previously we reported that more severe NPA may be present temporally compared to nasally in diabetic eyes (under review) – one wonders whether this may be related to differences in FD. In addition, we also

observed that FD decreased from the fovea to the far-periphery. This is in accordance with the observation that the peripheral retinal vessels supply a larger retinal area but with lower VD[25]. Analogously, in diabetic eyes, we found a more severe ischemic index (ISI) with increasing distance from the fovea[6]. Considering regional vascular differences in normal eyes may thus be of relevance to better understanding the distribution of pathologic features in the context of retinal vascular disease.

We also observed an age-related reduction of FD in the studied subjects. Consistent with our observation, Thomas *et al*[26] found that the FD at both the macula and OD was negatively correlated with age. Zhu *et al*[20] found that age was significantly associated with FD on color photographs in a Chinese Han population including 812 males and 1357 females. We hypothesized that this relationship may be due to the decrease in VD that occurs with age[27-28]. Consistent with this observation, a significant negative correlation of the FD with VD was reported by Ab Hamid *et al*[29]. Another possible explanation for the reduction in vessel FD with age may be the age-related lens opacity. Li *et al*[9] found that lens opacity had an independent effect on retinal vascular FD after adjusting for other confounding factors. Interestingly, although a relationship between FD and age was observed in the various retinal quadrants, posterior pole and mid-periphery, FD in the far-periphery appeared not to be influenced by age. If cataract or media opacity were a major factor, one would not expect the far-periphery to be spared from this phenomenon.

In the present study, a lower FD was also observed to be associated with a higher systolic BP. Similarly, Thomas *et al*[26] found that hypertensive subjects had significantly lower FD around the macula and optic nerve than healthy subjects. Sng *et al*[12] found that individuals with lower retinal FD tended to have uncontrolled treated or untreated hypertension. Kurniawan *et al*[30] found that higher blood pressure in children is associated with a smaller retinal FD. Liew *et al*[21] found that after adjustment for age and sex, mean FD was significantly lower in subjects with hypertension than without.

There are some limitations in our study. First, the sample size is somewhat limited. On other hand, recruiting large cohorts of normal individuals for invasive imaging is a challenge. Second, we did not specifically evaluate the severity of lens opacity. However, the influence from lens opacity and RE on FD has been proven to account for <3.5% of the variability in FD[9].

There are also several strengths to our study. First, differing from prior FA studies that have used the normal eyes of patients with unilateral retinal diseases as a control[31], we included only subjects in whom both eyes were normal, who were specifically recruited for this study[4]. Second, use of FA provided superior visualization of the microvasculature

compared to studies which used fundus images. Third, we obtained steered images and montaged them to allow visualization of the full retinal vasculature to the outer border of visible retina. Finally, the protocol for vessel segmentation used in this study was particularly designed for UWF SLO images and has been shown to achieve excellent vessel segmentation accuracy and low overall bias[16].

In summary, UWF FA imaging enables a global assessment of the complexity of the entire retinal vasculature including the far-periphery in healthy subjects. FD was non-uniformly distributed and decreased from the posterior pole to the far-periphery. Subjects with older age or high blood pressure appeared to have a lower FD; though, FD in the far-periphery appears not to be influenced by aging. This analysis in normal subjects may provide a useful reference for fractal properties of the retinal vasculature when analyzing the pathologies in the group of retinal vascular disease.

REFERENCES

1 Wessel MM, Nair N, Aaker GD, Ehrlich JR, D'Amico DJ, Kiss S. Peripheral retinal ischaemia, as evaluated by ultra-widefield fluorescein angiography, is associated with diabetic macular oedema. *Br J Ophthalmol* 2012;96(5):694-698.

2 Tan CS, Chew MC, van Hemert J, Singer MA, Bell D, Sadda SR. Measuring the precise area of peripheral retinal non-perfusion using ultra-widefield imaging and its correlation with the ischaemic index. *Br J Ophthalmol* 2016;100(2):235-239.

3 Price LD, Au S, Chong NV. Optomap ultrawide field imaging identifies additional retinal abnormalities in patients with diabetic retinopathy. *Clin Ophthalmol* 2015;9:527-531.

4 Singer M, SG, van Hemert J, Kuehlewein L, Bell D, Sadda SR. Ultra-widefield imaging of the peripheral retinal vasculature in normal subjects. *Ophthalmology* 2016;123(5):1053-1059.

5 Croft DE, van Hemert J, Wykoff CC, Clifton D, Verhoek M, Fleming A, Brown DM. Precise montaging and metric quantification of retinal surface area from ultra-widefield fundus photography and fluorescein angiography. *Ophthalmic Surg Lasers Imaging Retina* 2014;45(4):312-317.

6 Fan WY, Wang K, Ghasemi Falavarjani K, SG, Uji A, Ip M, Wykoff CC, Brown DM, van Hemert J, Sadda SR. Distribution of nonperfusion area on ultra-widefield fluorescein angiography in eyes with diabetic macular edema: DAVE study. *Am J Ophthalmol* 2017;180:110-116.

7 Masters BR. Fractal analysis of the vascular tree in the human retina. *Annu Rev Biomed Eng* 2004;6:427-452.

8 Zahid S, Dolz-Marco R, Freund KB, Balaratnasingam C, Dansingani K, Gilani F, Mehta N, Young E, Klifto MR, Chae B, Yannuzzi LA, Young

JA. Fractal dimensional analysis of optical coherence tomography angiography in eyes with diabetic retinopathy. *Invest Ophthalmol Vis Sci* 2016;57(11):4940-4947.

9 Li HT, Mitchell P, Liew G, Rochtchina E, Kifley A, Wong TY, Hsu W, Lee ML, Zhang YP, Wang JJ. Lens opacity and refractive influences on the measurement of retinal vascular fractal dimension. *Acta Ophthalmol* 2010;88(6):e234-e240.

10 Mainster MA. The fractal properties of retinal vessels: embryological and clinical implications. *Eye (Lond)* 1990;4(Pt 1):235-241.

11 Kim AY, Chu ZD, Shahidzadeh A, Wang RK, Puliafito CA, Kashani AH. Quantifying microvascular density and morphology in diabetic retinopathy using spectral-domain optical coherence tomography angiography. *Invest Ophthalmol Vis Sci* 2016;57(9):OCT362-OCT370.

12 Sng CC, Wong WL, Cheung CY, Lee J, Tai ES, Wong TY. Retinal vascular fractal and blood pressure in a multiethnic population. *J Hypertens* 2013;31(10):2036-2042.

13 Silva PS, Dela Cruz AJ, Ledesma MG, van Hemert J, Radwan A, Cavallerano JD, Aiello LM, Sun JK, Aiello LP. Diabetic retinopathy severity and peripheral lesions are associated with nonperfusion on ultrawide field angiography. *Ophthalmology* 2015;122(12):2465-2472.

14 Silva PS, Cavallerano JD, Sun JK, Soliman AZ, Aiello LM, Aiello LP. Peripheral lesions identified by mydriatic ultrawide field imaging: distribution and potential impact on diabetic retinopathy severity. *Ophthalmology* 2013;120(12):2587-2595.

15 Escudero-Sanz I, Navarro R. Off-axis aberrations of a wide-angle schematic eye model. *J Opt Soc Am A Opt Image Sci Vis* 1999;16(8): 1881-1891.

16 Pellegrini E, Robertson G, Trucco E, MacGillivray TJ, Lupascu C, van Hemert J, Williams MC, Newby DE, van Beek E Jr, Houston G. Blood vessel segmentation and width estimation in ultra-wide field scanning laser ophthalmoscopy. *Biomed Opt Express* 2014;5(12):4329-4337.

17 Fan WY, Nittala MG, Fleming A, Robertson G, Uji A, Wykoff CC, Brown DM, van Hemert J, Ip M, Wang K, Falavarjani KG, Singer M, SG, Sadda SR. Relationship between retinal fractal dimension and nonperfusion in diabetic retinopathy on ultrawide-field fluorescein angiography. *Am J Ophthalmol* 2020;209:99-106.

18 Avakian A, Kalina RE, Sage EH, Rambhia AH, Elliott KE, Chuang EL, Clark JI, Hwang JN, Parsons-Wingerter P. Fractal analysis of region-based vascular change in the normal and non-proliferative diabetic retina. *Curr Eye Res* 2002;24(4):274-280.

19 Tălu S. Fractal analysis of normal retinal vascular network. *Oftalmologia* 2011;55(4):11-16.

20 Zhu PL, Huang F, Lin F, Li QW, Yuan Y, Gao ZH, Chen FL. The relationship of retinal vessel diameters and fractal dimensions with blood pressure and cardiovascular risk factors. *PLoS One* 2014;9(9):e106551.

21 Liew G, Wang JJ, Cheung N, Zhang YP, Hsu W, Lee ML, Mitchell P, Tikellis G, Taylor B, Wong TY. The retinal vasculature as a fractal: methodology, reliability, and relationship to blood pressure. *Ophthalmology* 2008;115(11):1951-1956.

22 Somfai GM, Tátrai E, Laurik L, Varga BE, Ölvedy V, Smiddy WE, Tchitnga R, Somogyi A, DeBuc DC. Fractal-based analysis of optical coherence tomography data to quantify retinal tissue damage. *BMC Bioinformatics* 2014;15:295.

23 Salz DA, Witkin AJ. Imaging in diabetic retinopathy. *Middle East Afr J Ophthalmol* 2015;22(2):145-150.

24 Uji A, Balasubramanian S, Lei JQ, Baghdasaryan E, Al-Sheikh M, Sadda SR. Choriocapillaris imaging using multiple en face optical coherence tomography angiography image averaging. *JAMA Ophthalmol* 2017;135(11):1197-1204.

25 Fan WY, Uji A, Borrelli E, Singer M, SG, van Hemert J, Sadda SR. Precise measurement of retinal vascular bed area and density on ultra-wide fluorescein angiography in normal subjects. *Am J Ophthalmol* 2018;188:155-163.

26 Thomas GN, Ong SY, Tham YC, Hsu W, Lee ML, Lau QP, Tay W, Alessi-Calandro J, Hodgson L, Kawasaki R, Wong TY, Cheung CY. Measurement of macular fractal dimension using a computer-assisted program. *Invest Ophthalmol Vis Sci* 2014;55(4):2237-2243.

27 Leung H, Wang JJ, Rochtchina E, Tan AG, Wong TY, Klein R, Hubbard LD, Mitchell P. Relationships between age, blood pressure, and retinal vessel diameters in an older population. *Invest Ophthalmol Vis Sci* 2003;44(7):2900-2904.

28 Shahlaee A, Samara WA, Hsu J, Say EA, Khan MA, Sridhar J, Hong BK, Shields CL, Ho AC. *In vivo* assessment of macular vascular density in healthy human eyes using optical coherence tomography angiography. *Am J Ophthalmol* 2016;165:39-46.

29 Ab Hamid F, Che Azemin MZ, Salam A, Aminuddin A, Mohd Daud N, Zahari I. Retinal vasculature fractal dimension measures vessel density. *Curr Eye Res* 2016;41(6):823-831.

30 Kurniawan ED, Cheung N, Cheung CY, Tay WT, Saw SM, Wong TY. Elevated blood pressure is associated with rarefaction of the retinal vasculature in children. *Invest Ophthalmol Vis Sci* 2012;53(1):470-474.

31 Kaneko Y, Moriyama M, Hirahara S, Ogura Y, Ohno-Matsui K. Areas of nonperfusion in peripheral retina of eyes with pathologic myopia detected by ultra-widefield fluorescein angiography. *Invest Ophthalmol Vis Sci* 2014;55(3):1432-1439.